Geobios 72–73 (2022) 1–11

Contents lists available at ScienceDirect

Geobios

journal homepage: www.elsevier.com/locate/geobio

Faunal evidence of the 1755 Lisbon Tsunami in Gibraltar (S Iberian Peninsula) ☆

Manuel Abad [a,b,*], María José Clemente [c], María Luz González-Regalado [c], Francisco Ruiz [c,d], Joaquín Rodríguez Vidal [c,d], Luis Miguel Cáceres [c,d], Tatiana Izquierdo [a], Juan Carlos Pérez Quintero [e], Josep Tosquella [c], Manuel Pozo [f], Paula Gómez [c,d], Antonio Toscano [c], Verónica Romero [c], Marta Arroyo [c], Gabriel Gómez [c]

[a] Departmento de Biología y Geología, Física y Química Inorgánica, ESCET, Universidad Rey Juan Carlos, c/Tulipán, s/n, 28933 Móstoles, Spain
[b] Corporación de Investigación y Avance de la Paleontología e Historia Natural de Atacama -CIAHN-, Avenida Prat 58, Caldera, Atacama, Chile
[c] Departmento de Ciencias de la Tierra, Universidad de Huelva, Avenida 3 de marzo, 21071 Huelva, Spain
[d] Research Center in Historical, Cultural and Natural Heritage, Universidad de Huelva, Avenida 3 de marzo, 21071 Huelva, Spain
[e] Departmento de Ciencias Integradas, Universidad de Huelva, Avenida 3 de marzo, 21071 Huelva, Spain
[f] Departamento de Geología y Geoquímica, Universidad Autónoma de Madrid, Avda. Francisco Tomas y Valiente 7, 28049 Madrid, Spain

ARTICLE INFO

Article history:
Received 17 September 2021
Accepted 14 June 2022
Available online 8 July 2022

Keywords:
Sedimentary facies
Macrofauna
Foraminifera
1755 Lisbon Tsunami
Gibraltar
S Iberian Peninsula

ABSTRACT

This paper analyzes the first systematic faunal record of the 1755 Lisbon tsunami in the Mediterranean. On the basis of sedimentological and paleontological features, the sedimentary record of a core collected in Gibraltar was divided into six sedimentary facies, with a paleoenvironmental evolution from a shallow marine paleoenviroment to an increasingly restricted lagoon. This record includes a bioclastic layer deposited by the 1755 Lisbon tsunami and characterized by an erosive base, presence of basal rip-up clasts and abundant shell debris composed by marine and brackish molluscs. The paleoenvironmental reconstruction derived from the foraminiferal analysis is congruent with that inferred from the sedimentary and the macrofaunal reconstructions, with the introduction of brackish species into the innermost, intertidal areas of a confined lagoon. This paleontological record is the first faunal evidence of the 1755 Lisbon tsunami in the Mediterranean.

1. Introduction

Recent decades have witnessed an exponential increase in research on tsunamis and their geological record, largely due to the very serious consequences (deaths, economic losses, geomorphological changes, possible recurrence periods) of the 2004 Indian Ocean tsunami, the 2009 South Pacific tsunami, the 2010 Maule tsunami and the 2011 Tohoku tsunami. Pioneer papers focused mainly on tsunami sedimentology and geomorphology (Coleman, 1968, 1978; Dawson, 1994, 1996, 2003), while the aforementioned tsunamis caused a boom in both general (e.g., Dawson and Stewart, 2007; Bourgueois, 2009; Chagué-Goff et al., 2011; Engel et al., 2020; Costa and Andrade, 2020) and specialized (e.g., Chagué-Goff et al., 2017; Prastowo et al., 2017; Donadio et al., 2020) reviews. Most of the published research analyzes the geological record of these tsunamis and others that occurred during the Holocene, but there is also evidence of tsunamis during the Paleozoic (Jarochowska and Munnecke, 2015), Mesozoic (Matysik and Szulc, 2019), Cenozoic (Le Roux et al., 2008) and the limits between these eras (Bourgueois, 1994; Tohver et al., 2018).

The paleontological record has played an important role in the characterization of the sedimentary layers associated with these high-energy events. Several groups have proven to be excellent tsunamis tracers, such as bivalves (Kitamura et al., 2018), diatoms (Dura and Hemphill-Hale, 2020), ostracods (Ruiz et al., 2010a), coccolithophores (Paris et al., 2010) or pollen (Pilarczyk et al., 2014). However, foraminifera have monopolized most of the publications on this topic (e.g., Mamo et al., 2009; Hawkes, 2020). The analysis of their assemblages and taphonomy in coastal cores allows the identification of tsunami layers, in conjunction with facies interpretation (Nagendra et al., 2005; Finger, 2018; Pilarczyk et al., 2019).

On the morning of November 1, 1755, the southwestern coasts of Europe were ravaged by a devastating earthquake (M_w~8,5 ± 0,3; Solares and Arroyo, 2004) and its associated

☆ Corresponding editor: Frédéric Quillévéré.
* Corresponding author.
E-mail address: manuel.abad@urjc.es (M. Abad).

https://doi.org/10.1016/j.geobios.2022.07.003
0016-6995/

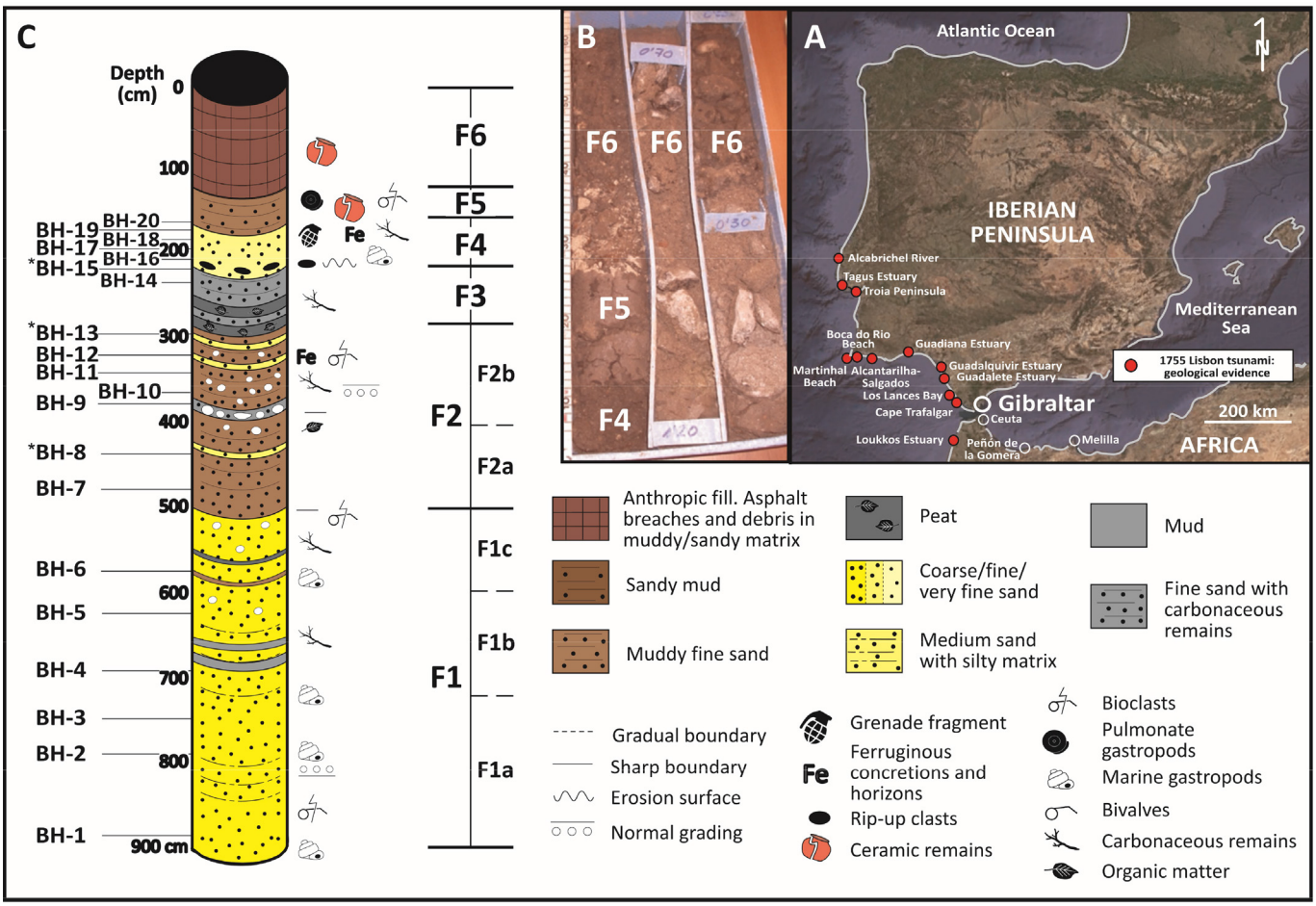

Fig. 1. **A**. Map location of geological evidences of the 1755 Lisbon Tsunami in the southern Iberian Peninsula. **B**. Core BH: photography of the uppermost three facies. **C**. Log of core BH with indication of samples' location. Asterisks indicate the dated samples.

tsunami, with waves up to 15 m high (Baptista et al., 1998). Geological evidence of this tsunami is widely recognized in the Atlantic coast of Spain, Portugal or Morocco (Font et al., 2013; Ruiz et al., 2013; El Talibi et al., 2016; Fig. 1(A)). However, the effects of this event on the adjacent Mediterranean littoral are little know so far.

This paper analyzes the sedimentary facies and foraminiferal record of a sediment core obtained from the Rock of Gibraltar (southern Iberian Peninsula). Its main objectives are: (*i*) to reconstruct the Late Holocene paleoenvironmental evolution of the northern part of this Rock; and (*ii*) to determine if the 1755 Lisbon Tsunami flooded this Mediterranean zone.

2. Geological setting and historical data

The Rock of Gibraltar is located at the southern tip of the Iberian Peninsula, near the western entrance to the Mediterranean Sea (Fig. 1(A)). The Rock is part of a narrow 6 km^2 peninsula, with three main regions (Rose and Rosenbaum, 1990): (*i*) the Isthmus, with Holocene sediments that join the Rock to the mainland; (*ii*) the Main Ridge (426 m heigth), formed by Early Jurassic limestones and dolomites; and (*iii*) the Southern Plateau, a staircased slope between 130 m and Present sea level (Fig. 2).

The Isthmus was occupied by an old lagoon until the end of the 19th century (Fig. 2(B): The Inundation). This lagoon was progressively isolated by the growth of a sandy barrier and only had a natural opening towards the sea in 1755, according to the cartography available in the Gibraltar Museum. A 1760 map does not show evidence of washover fans around the lagoon (Rodríguez-Vidal et al., 2011), so it is reasonable to think that a possible tsunami deposit derived from the 1755 Lisbon Tsunami could only have been deposited at its bottom or its intertidal areas. This previous historical investigation justifies the place chosen for the extraction of the selected core. Other reasons also support the choice of the coring site are: (*i*) the natural opening of this lagoon would allow the entry of the tsunami, being open to the west; and (*ii*) this core is located near this old opening.

3. Material and methods

Core BH (Fig. 1(B, C); 9 m length) was collected at the southern end of the Isthmus, within the area historically occupied by The Inundation lagoon. An initial geological study of this core included the uppermost 3 m, although the paleontological record was analyzed very briefly, with the inclusion of a few species of the main groups (mainly molluscs) whitout the application of statistical methods (Rodríguez-Vidal et al., 2011). In this new paper, the different sedimentary facies were differentiated according to their lithology, sedimentary structures, boundaries, macrofauna, plant remains and other visible elements (Fig. 1(C)). In a second phase, a Malvern Mastersizer 2000 (Malvern Instruments Ltd. Malvern, UK) was used to determine the particle size of sediments <2 mm in each facies. In addition, the molluscan assemblages of each facies were determined. The taxonomic determination was based on a comparison with the World Register of Marine Species (WoRMS) and Gómez (2017).

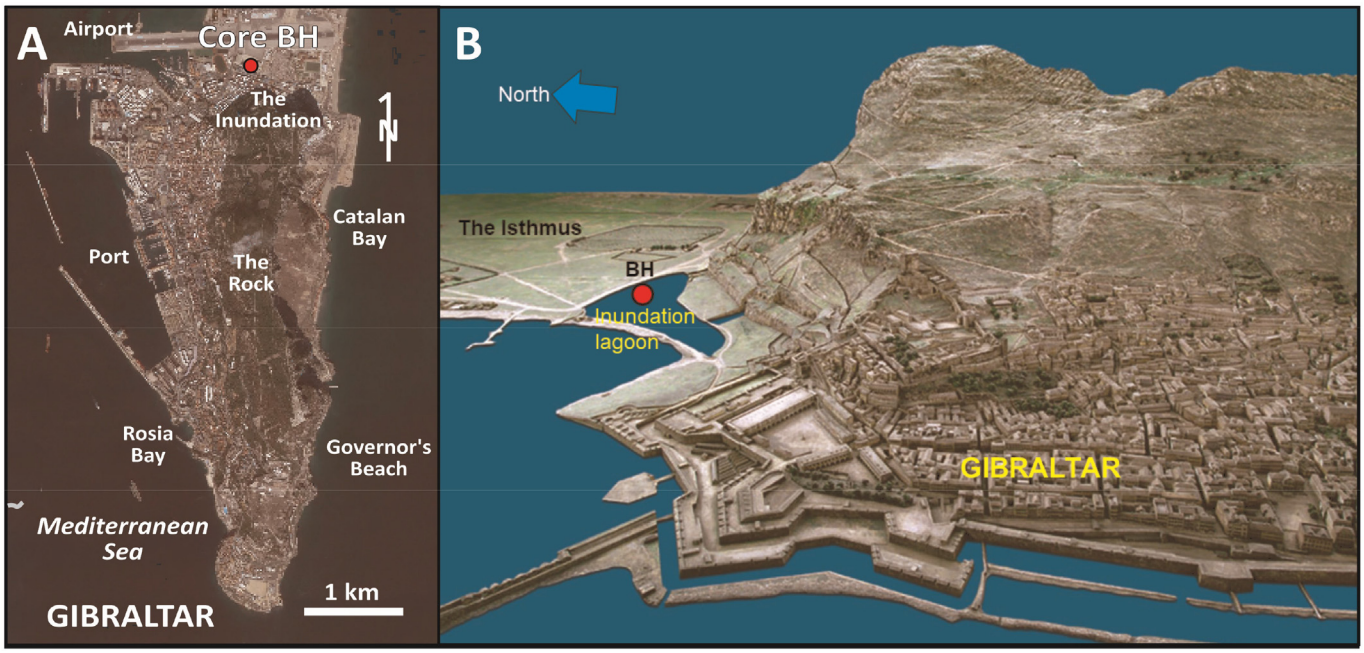

Fig. 2. **A**. Main geographical features of the Rock of Gibraltar (see text for details), with location of core BH. **B**. Reconstruction of the Inundation lagoon area. Oblique view of the North Face of the Rock of Gibraltar, with a good perspective of the ancient lagoon and the BH borehole location (red dot). Figure based on the three-dimensional model of the Rock, realized by Lt. Charles Warren in 1865-1868.

Twenty samples (20 g each) were selected for their foraminiferal analysis according to: (*i*) the distribution of the sedimentary facies; (*ii*) their boundaries; and (*iii*) the mollusc distribution. Samples were wet sieved (63 μm mesh) and dried in an oven at 70°C. Total populations of these microorganisms were extracted from each one of them and the number of species of each sample was calculated. The taxonomic determination was based on a comparison with the World Register of Marine Species (WoRMS) and numerous specialized publications on recent foraminifera of adjacent areas (e.g., Villanueva, 1995; González-Regalado et al., 2001; Papaspyrou et al., 2013). The five main species were photographed with the electron microscope of the Central Research Services (University of Huelva, Spain). The abundance of each species or assemblage in each sample was defined as follows: very rare (1 individual/20 g), rare (2-5 individuals/20 g), frequent (6-10 individuals/20 g), abundant (11-20 individuals/20 g) and very abundant (>20 individuals/20 g).

The nine most abundant species were used to carry out a statistical analysis, which represents 96% of the extracted benthic foraminifera. This statistical treatment was conducted with procedures developed in the R program (R-core team, 2019). This analysis included the calculation of their correlation coefficients and a double cluster analysis (R-mode and Q-mode). In both cases, results are based on raw abundances, i.e., untransformed count data. The R-mode cluster analysis was initially applied based on the measure of similarity of the Pearson correlation coefficient, with the whole union (furthest neighbor) method as the agglomeration algorithm. In addition, the percentage of homogeneity was calculated. For the Q-mode cluster analysis, we considered the Manhattan (i.e., Minkowski of order 1) distance, since observations (samples) have many zeros (species not present) and variables (number of individuals of each species) are counts. This distance between two samples is defined as the sum of absolute differences in the number of individuals of each of the species: $d(u, v) = \sum_i |u_i - v_i|$. In the resulting dendrogram, the clustering height or distance is the value of the criterion associated with the clustering method for the particular agglomeration. In order to obtain a more informative and illustrative plot, the R Program function "plot.hclust" performs a distance transformation to adapt the height of the plot.

Three radiocarbon dates were obtained at Beta Analytic Laboratory (Miami, USA). These dates were calibrated with the program IntCal09.14c and the final results are expressed as the highest probable age of the 2 sigma calibrated range. In addition, some grenade fragments were extracted at ~1.8 m depth and associated historical data are interesting to date the age of the intermediate facies of core BH.

4. Results

4.1. Sedimentary facies and macrofauna

Six sedimentary facies have been identified in core BH, with different subfacies distinguished by their malacological content (Fig. 1(C)).

Facies 1 (Fig. 1(B): 9-5 m depth) is made up of yellowish, massive fine and medium sands. Three subfacies have been defined by their associated macrofauna:

- F1a (9-7.2 m depth), characterized by the presence of numerous valves and shells of marine molluscs such as gastropods and bivalves (Table 1);
- F1b (7.2-6 m depth), composed of well sorted medium sands with very scarce macrofauna;
- F1c (6-5 m depth), which includes numerous remains of annelids, echinoderms, crab clamps and undifferentiated fragments of gastropods.

Facies 2 (F2: 5-3 m depth) shows massive to slightly bedded muddy very fine sands with abundant molluscs near the base (subfacies F2a: 5-4 m depth) and numerous plants remains and sharp quartz fragments towards the top (subfacies F2b: 4-3 m depth).

Table 1
Foraminifera abundance and diversity in the analyzed samples.

Facies	Texture	Sedimentary structures	Subfacies	Gastropods	Bivalves	Other features	Main foraminiferal species
F1	Fine and medium sand	Massive	F1a	*Steromphala divaricata* (M)	*Acanthocardia aculeata* (M)		*Ammonia beccarii*
					Macomangulus tenuis (M)		*Ammonia tepida* *Elphidium crispum*
			F1b	Very scarce			*Elphidium advenum*
			F1c	Undifferentiated fragments		Remains of annelids, echinoderms and crab clamps	*Elphidium crispum* *Quinqueloculina vulgaris* *Ammonia beccarii*
							Ammonia tepida *Quinqueloculina vulgaris*
F2	Muddy very fine sands	Massive or parallel lamination	F2a	*Calliostoma zizyphinum* (M)	*Parvicardium scriptum* (M)		*Ammonia beccarii*
				Tritia neritea (M) *Tritia incrassata* (M) *Bittium reticulatum* (M)	*Diplodonta rotundata* (M) *Chamelea gallina* (M) *Macomangulus tenuis* (M)		*Ammonia tepida* *Elphidium advenum*
			F2b	*Hydrobia acuta* (B)		Plant remains	Very scarce or absent *Elphidium crispum*
F3	Alternance of pear layers and fine sands	Parallel lamination		*Hydrobia acuta* (B)		Numerous carbonaceous remains	Very scarce or absent *Ammonia tepida*
F4	Medium and fine sands	Basal erosion surface Peaty and muddy rip-up clasts		*Calliostoma laugieri* (M)	Undifferentiated fragments	Reddish oxidation horizon with carbonaceous remains	Almost exclusively *Ammonia tepida*
				Jujubinus striatus (M) *Tricolia tenuis* (M) *Peringia ulvae* (B)			
F5	Muddy sands			*Xerotricha apicina* (P)		Ceramic remains	Scarce. Mainly *Elphidium crispum* and *Ammonia* spp.
				*Theba pisana (*P)			
F6	Asphalt breccias and debris					Ceramic remains	

Table 2
Core BH. Vertical distribution of benthic foraminifera in the twenty studied samples (20 g/sample). The number of individuals per gram has been rounded to the nearest whole number.

Facies	F5	F4				F3		F2					F1				F1a		
Subfacies								F2b			F2a		F1c	F1b					
Species/Samples	BH-20	BH-19	BH-18	BH-17	BH-16	BH-15	BH-14	BH-13	BH-12	BH-11	BH-10	BH-9	BH-8	BH-7	BH-6	BH-5	BH-4	BH-3	BH-2	BH-1
Adelosina mediterranensis			1																	
Adelosina pulchella		1							2											3
Ammonia beccarii	2												7	18	20	2	2	55	35	52
Ammonia tepida	2	6	12	37	37	2				1		2	60	68	20			48	6	35
Cribroelphidium excavatum																				3
Cycloforina contorta																	3	1		
Elphidium aculeatum														6	6	3	8	2	4	
Elphidium advenum	1									3			8	11	14	12	10	13	14	3
Elphidium complanatum												3								6
Elphidium crispum	8								3	9	2	1	8	6	12	15	53	15	11	36
Elphidium macellum												3						2		20
Haynesina germanica													2					1	1	3
Lenticulina sp.	1			2																3
Quinqueloculina seminulum										1			3	4	5	2	4	1		
Quinqueloculina vulgaris				2						3	2		2	3	15	8	12	7	6	11
Siphonaperta lucida													2							
Triloculina oblonga														3						1
Triloculina trigonula										1							2		2	4
Number of individuals/20 g	14	7	13	41	37	2			5	18	4	9	92	119	92	42	94	145	79	180
Number of individuals/g	1	<1	1	2	2	<1			<1	1	<1	<1	5	6	5	2	5	7	4	9
Number of species	5	2	2	3	1	1			1	6	2	4	8	8	7	7	8	10	8	13

Marine gastropods (mainly *Calliostoma zizyphinum* (Linnaeus, 1758) and *Tritia* spp.) and bivalves (mainly *Chamelea gallina* (Linnaeus, 1758)) are dominant in F2a (Table 1), while small brackish gastropods (*Hydrobia acuta* (Draparnaud, 1805) and *Peringia ulvae* (Pennant, 1777)) are frequent in F2b.

Facies 3 (F3: 3-2.12 m depth) presents alternating peat layers and peaty fine sands (5-15 cm thickness) and peaty fine sands with numerous carbonaceous remains. Only a few shells of *H. acuta* have been collected in this facies.

Facies 4 (F4: 2.15-1.8 m depth) consists of quartz-rich medium and fine sands with scarce percentages of silts and clays. The basal contact of F4 is a sharp erosion surface drapped by irregular rip-up clasts of peat derived from F3. Fragmented shells of marine (mainly *Jujubinus striatus* (Linnaeus, 1758)) and brackish (*P. ulvae*) are frequent. This facies includes a reddish oxidation horizon (190 cm depth) with numerous carbonaceous remains.

Facies 5 (F5: 1.8-1.5 m depth) is made up of greyish, muddy sands with debris, frequent ceramic remains and numerous small shells of pulmonate gastropods (Table 1).

Last, **Facies 6** (F6) relates to the uppermost 1.5 m of the core. It is composed of numerous asphalt breccias and debris.

4.2. Foraminifera and facies

A total of 993 benthic foraminifera were collected from the twenty selected samples, belonging to 10 genera and 18 species (Table 2). These microorganisms are very abundant (>75 individuals/20 g) in some samples of F1a and F2a, while they are very scarce (<1 individual/gram) or even dissapear in F2b, F3 and F5. The number of species ranges from 1 to 8 in most samples (Table 2; Fig. 3) and only more than ten species have been extracted in the basal samples of F1a.

Five species represent more than 87% of the foraminifera picked (Fig. 3): *Ammonia tepida* (Cushman, 1926) (33.8%), *Ammonia beccarii* (Linnaeus, 1758) (19.4%), *Elphidium crispum* (Linnaeus, 1758) (18%), *Elphidium advenum* (Cushman, 1922) (9%), and *Quinqueloculina vulgaris* d'Orbigny, 1826 (7.2%). These five species are abundant in F1a, F1c and F2a, while the last three species are dominant in F1b and, to a lesser extent, in F2b. F4 is characterized by a remarkable increase in *A. tepida* in its basal layer (2.15-2 m depth) and a significant decrease of this species towards the top of this facies (Table 1; Fig. 3).

In general, the foraminifera are well preserved, with no evidence of abrasion or fragmentation, with only some exceptions found in two facies: (*i*) F1b, with frequent fragmented elphidids of large size and numerous Miliolidae with loss of the last chamber; and (*ii*) basal samples of F4, with shattered or fragmented specimens of *A. tepida* (around 30% of the total specimens).

4.3. Statistical analysis

Three foraminiferal assemblages can be differentiated according to the correlation coefficient matrix (Table 3) and the R-mode cluster analysis (Fig. 4(A,B)), with an adequate percentage of homogeneity (53.37% for k = 3 groups):

- **Assemblage 1** (*Ammonia beccarii-Elphidium macellum* (Fichtel and Moll, 1798)-*Triloculina trigonula* (Lamarck, 1804)), dominant in F1a (39-47%) and the basal sample of F2b, although this sample contains a scarce number of individuals (Table 2);
- **Assemblage 2** (*A. tepida*), abundant in F2a (57-65%) and the basal two samples of F4 (90-100%);
- **Assemblage 3** (*E. crispum-Elphidium aculeatum* (d'Orbigny, 1846)-*E. advenum-Quinqueloculina seminulum* (Linnaeus, 1758)-*Q. vulgaris*), very abundant in F1b (40-87 individuals/20 g;

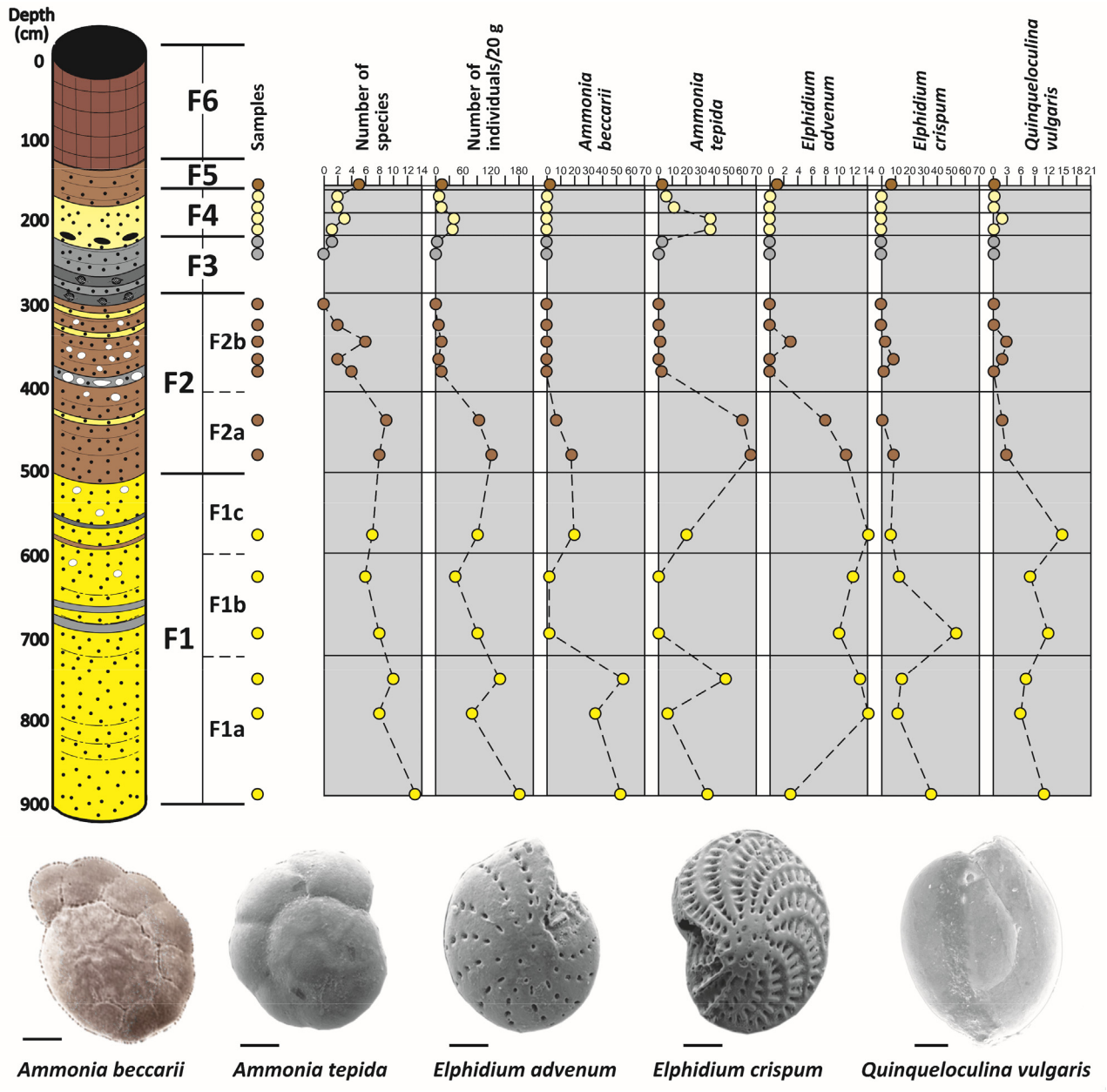

Fig. 3. Diversity, density and abundance (individuals/20 g) of the main benthic foraminifera species of core BH.

Table 3
Correlation matrix between the nine main species. Bold: p < 0.01; underlined: p < 0.05.

	AB	AT	EA	ED	EC	EM	QS	QV	TT
Ammonia beccarii (AB)	1								
Ammonia tepida (AT)	0.47	1							
Elphidium aculeatum (EA)	0.26	0.15	1						
Elphidium advenum (ED)	**0.57**	0.34	**0.8**	1					
Elphidium crispum (EC)	0.42	0.03	**0.6**	0.48	1				
Elphidium macellum (EM)	**0.61**	0.2	-0.15	-0.05	0.46	1			
Quinqueloculina seminulum (QS)	0.12	0.38	**0.81**	**0.72**	0.46	-0.16	1		
Quinqueloculina vulgaris (QV)	**0.57**	0.13	**0.72**	**0.74**	**0.77**	0.36	**0.65**	1	
Triloculina trigonula (TT)	**0.55**	0.31	0.43	0.33	**0.63**	**0.64**	0.24	0.47	1

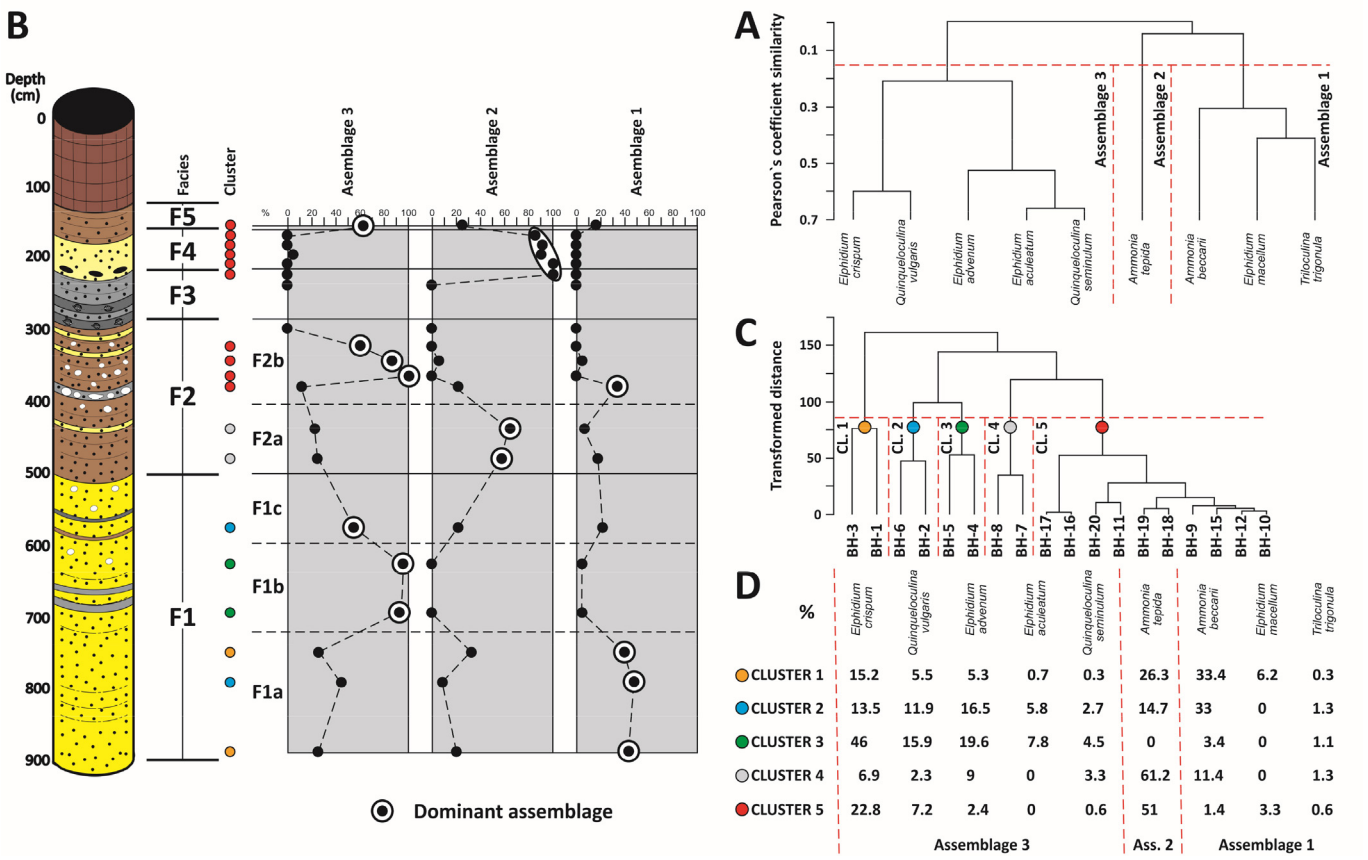

Fig. 4. Statistical analyses based on benthic foraminifera. **A**. Species group R-mode cluster analysis showing main foraminiferal assemblages. **B**. Vertical variation of relative abundance of the three foraminiferal assemblages. **C**. Sample group Q-mode cluster analysis. **D**. Relative abundances of the main foraminiferal species in the five sample groups.

56-95%) and dominant in most samples of F2b (3-16 individuals/20 g; 60-100%) and F5 (9 individuals/20 g; 64%).

The Q-mode analysis grouped the studied samples into five groups (Fig. 4(C,D)):

- **Cluster 1** includes two samples of F1a characterized by the highest diversity of core BH (Fig. 3: 10-13 species/sample) and the highest number of individuals (Fig. 3: 145-180 individuals/20 g). In this cluster, Assemblage 1 is slightly dominant (mean M = 40.1%) over Assemblages 3 (M = 27%) and 2 (M = 26.3%), with *A. beccarii* as the most abundant species (M = 33.4%);
- *beccarii* is also abundant in **cluster 2** (two samples; F1a-F1c) together with elphidids, but Assemblage 3 is clearly dominant (M = 50.4%) in these samples;
- Elphidids (M = ~70%) are the most representative group of **cluster 3**, which includes the two samples of F1b;
- Diversity of **cluster 4** (F2a: two samples) ranges from 7 to 8 species per sample, with very abundant individuals (92-119 individuals/20 g). This cluster is dominated by *A. tepida* (Assemblage 2; M = 61,2%), with *Ammonia beccarii* (M = 11.4%) and *E. advenum* (M = 9%) as secondary species;
- **Cluster 5** (F2b-F3-F4-F5) groups ten less similar samples all characterized by lower diversities (≤5 species/sample) and densities (2-41 individuals/20 g) and a predominance of Assemblage 3 (F2b-F5) or Assemblage 2 (F3-F4). The highest number of individuals was picked in the basal samples of F4 (Table 1: 37-41 individuals/20 g), almost all of them belonging to *A. tepida* (~95%).

4.4. Dating

The age of the different facies can be approximately deduced from the three dates obtained (Table 3) and the extracted artillery fragment located in the top of F4. F1 was deposited during the lower-middle Holocene (>6 kyr BP), while a middle Holocene age (6-4.1 kyr BP) is inferred for F2. The age of F3 is between ca. 4.1 kyr BP and ca. 2.8 kyr BP although the evident erosional surface between this facies and F4 points to a later partial loss of part of the F3 peaty sediments. Finally, the projectile fragment found in the top of F4 corresponds with a 6-pound hand-grenade which was used during the Great Siege (1779-1781), a hostile engagement between Great Britain and Spain.

5. Discussion

5.1. Facies interpretation: paleoenvironmental evolution

During the Late Pleistocene-Early Holocene, an open lagoon (Fig. 5: F1a) occupied the Isthmus of Gibraltar, as can be deduced from both the macrofauna and the microfauna. The common shell *S. divaricata* is a shallow-water species distributed throughout the Mediterranean Sea and along the coasts of the Black Sea (Anistratenko, 2005; Templado, 2011). The high percentages of Assemblages 1 and 3 (Fig. 4) points to an intertidal or littoral areas, probably linked to a barrier beach with sandy bottoms and high-energy conditions, while the moderate density of Assemblage 2 (Table 2: up to 48 specimens/20 g) indicate partial salinity-stressed conditions and the presence of a source of freshwater

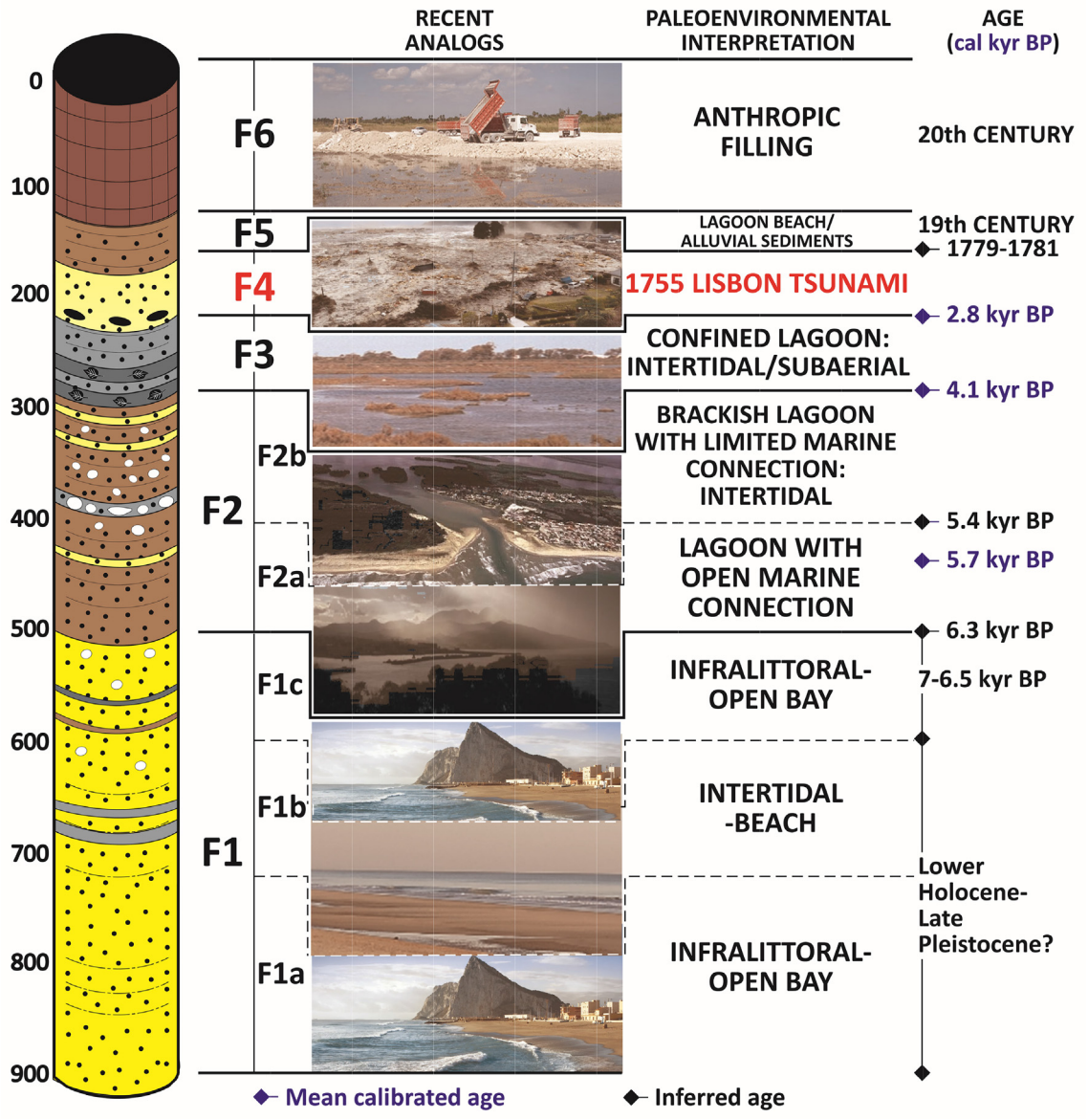

Fig. 5. Paleoenvironmental reconstruction of core BH.

Table 4
Database of ^{14}C results.

Sample	Depth (cm)	Laboratory	Laboratory number	Type	Uncalibrated age (yr BP)	Error	$\partial^{13}(^{0}/_{00})$	Calibrated age (yr BP)	Mean calibrated age (kyr)
BH-15	215	Beta Analytic	Beta-290903	Peat	2680	30	-28.0	2850-2750	2.8
BH-13	300	Beta Analytic	Beta-290904	Peat	3770	40	-27.9	4290-3980	4.1
BH-8	440	National Accelerator Center	CNA-4260	Shell	5340	35	-11.5	5830-5600	5.7

owing to the abundance or *Ammonia* spp. (Melis, 2013; Gupta et al., 2019).

Transition to F1b is characterized by the disappearance of *Ammonia* spp. and the presence of fragmented specimens of elphidids and miliolids (Fig. 3). The sandy sediments, the presence of reworked taxa and the abundance of Assemblage 3 (Fig. 4: >90%) are characteristics of beach environments (Fiorini, 2004; Al-Wosabi et al., 2017). The increasing presence of both Assemblages 1 and 2 in F1c would indicate a return to the previous paleoenvironmental conditions (e.g., F1a), which coincided with the maximum of the MIS-1 transgression (7-6.5 kyr BP; Zazo et al., 1994; Kumar and Barnejee, 2016).

Two dates were obtained in F2 at depths of 3.0 m and 4.4 m, respectively (Table 4), and consequently a mean sedimentation rate of ~0.875 mm/yr can be roughly deduced for this facies. An extrapolation of this rate to the whole F2 indicates that: (*i*) subfacies F2a began to deposit at ca. 6.3 kyr and confirms the previously assumed age for F1c; and (*ii*) the age of the boundary between F2a and F2b is ca. 5.4 kyr BP (Fig. 5).

The abundant macrofauna of F2a is typically marine, with numerous shells and valves of bivalves (*Parvicardium*, *Diplodonta*, *Chamelea*, *Macomangulus*) and gastropods (*Calliostoma*, *Tritia*, *Bittium*) that generally live together in sandy substrates from the mesolittoral zone to a depth of 30 m in southwestern Spain

(Gómez, 2017). This mollusc assemblage coincides with a predominance of *A. tepida* (Assemblage 2; 60-68 individuals/20 g; 57-65%) and a secondary presence of Assemblage 3 (22-25%). This foraminiferal population has been observed in sandy-silty intertidal to subtidal zones of ancient and current partially confined lagoons, gulfs, bays and other paralic environments (Debenay et al., 1998; Murray, 2006; Guerra et al., 2020). This faunal concurrence and the low foraminiferal diversity (Table 2: 8 species/sample) points to the presence of a lagoon with a broad marine connection between a. 6.3 kyr BP and ca. 5.4 kyr BP in the current Isthmus of Gibraltar. Brackish gastropods (*H. acuta*, *P. ulvae*) and rare specimens of Assemblage 3 (elphidids, miliolids) constitute the scarce faunal record of the basal samples of F2b, while these taxa dissapear towards the top of this subfacies (Table 2). This record is also characteristic of a brackish, more confined lagoon conditions in relation to F2a (Avramides et al., 2014; Chevalier et al., 2014), with a progressive reduction of marine inputs.

Only a few specimens of *H. acuta* were collected in F3 (Fig. 4: ca. 4.1-2.8 kyr BP), within several fine peaty layers. This gastropod is a typical lagoonal species (Dezileau et al., 2016) and the disappearance of foraminifera at the base of F3 (Table 2; Fig. 3) confirms the presence of an increasing confined lagoon. The mean sedimentation rate decreases slightly (0.65 mm/yr) during this period, as in other estuaries and lagoons of southwestern Spain (Lario et al., 2002).

The following geological characteristics of F4 are very similar to those of tsunami deposits (Dawson, 2007; Dawson and Stewart, 2007; Engel et al., 2020):

- an irregular erosive surface marks the contact between both facies;
- the basal part of F4 includes numerous peaty rip-up clasts from F3;
- grain size increases with respect to F3;
- numerous fragmented shells of marine gastropods are observed in the basal layers of this facies;
- frequent specimens of assemblage 2 were found in these layers, coming from the most external areas of the lagoon (e.g., F2a) by the tsunami waves that surpassed the sandy barriers that delimited it;
- the age of a sample located just below the limit with F3 (Table 4: ca 2.8 kyr BP) reveals a strong erosion of the latter facies, with the disappearance of about 2.6 kyr of geological record.

Finally, the presence of a fragment of a 6-pound hand-grenade used during the Great Siege (1779-1781) just above this facies would indicate that F4 comes from erosive action of the 1755 Lisbon Tsunami on the historical The Inundation lagoon.

F5 shows a faunal transition from a basal layer with scarce individuals of the three foraminiferal assemblages (Table 2) to an upper layer with frequent shells of pulmonate gastropods. This evolution would evidence the passage from a shallow intertidal zone or a beach to subaerial paleoenvironments (Morhange et al., 2000), which would later be covered by an anthropic filling (F6) during the 20th century.

5.2. Faunal evidence of the 1755 Lisbon tsunami: the Mediterranean emptiness

As already indicated above (see Introduction and Fig. 1(A)), numerous studies have analyzed the geological record of the 1755 Lisbon tsunami in southwestern Spain (Solares and Arroyo, 2004; Silva et al., 2017). This record includes, among others: (*i*) washover fans (Luque et al., 2002); (*ii*) exposed bioclastic ridges (Ruiz et al., 2004); (*iii*) bioclastic layers within marsh and lagoonal deposits (Ruiz et al., 2008; 2010b); (*iv*) boulder deposits (Whelan and Kelletat, 2005); (*v*) erosion of spits, beaches and barrier islands (Ruiz et al., 2013); and (*vi*) erosion of littoral foredunes and reactivation as transgressive dunes over the edge of inner estuarine marshes (Rodríguez-Vidal et al., 2011). The faunal record is a useful tracer of these tsunami deposits because tsunami waves caused the introduction of both lagoonal and marine species of molluscs (Cuven et al., 2013), foraminifera (Costa et al., 2012), ostracods (Ruiz et al., 2005) or diatoms (Quintela et al., 2016) into inland areas of alluvial plains, estuaries, marshes, barrier-islands or bays.

In relation to the 1755 Lisbon tsunami, some faunal features of the associated tsunamiites can be summarized (Dawson et al., 1995; Costa et al., 2012; Font et al., 2013; Cuven et al., 2013):

- the basal layer of these high-energy deposits contains usually a distinctive gravel-sized shell debris with abundant marine molluscs;
- sea-urchin radiols, fragmented diatoms, sponge spicules and even calcareous algae are also usually present in this layer;
- the foraminiferal record includes marine and/or brackish assemblages (elphidids, miliolids, inner shelf species), depending on the previous paleogeography and paleoenvironments;
- in some cases, the micropaleontological record even detected tsunami backwash, with the presence of brackish ostracods.

Nevertheless, there is a notable void in the adjacent Mediterranean area, although geological evidence of the 1755 Lisbon tsunami has been detected in very close Atlantic areas (Fig. 1(A)). The Moroccan tsunami catalog does not include any effect of this tsunami on the Mediterranean facade of this country (Kaabouben et al., 2009) and some Spanish sites and cities located in North Africa did not suffer the effects of this event (Fig. 1(A): Rock of Vélez de la Gomera, Melilla; Martínez Solares, 2001). In the Mediterranean, the unique geological record of this event was provided so far by Rodríguez-Vidal et al. (2011) in Gibraltar and includes the deposit of bioclastic sands in open crevices of Rosia Bay (Fig. 2(A, B)), among other evidences. Consequently, this paper represents the first faunal record of the 1755 Lisbon Tsunami in the Mediterranean Sea.

6. Conclusions

The multidisciplinary analysis (stratigraphy, sedimentology, macrofauna, foraminifera, dating) of a sediment core collected in the Rock of Gibraltar (S Iberian Peninsula) has made it possible to reconstruct the paleoenvironmental evolution of the isthmus that joins it to the mainland. During the Late Holocene, an open bay occupied this area, which was progressively confined until forming a restricted lagoon, historically called The Inundation. This gradual closure was accompanied by a decreasing grain size, the apparition of peaty layers and the disappearance of the benthic foraminifera. During the 18th century, this lagoon was in an advanced state of clogging, according to historical data. On the morning of November 1, 1755, the study site was flooded by the 1755 Lisbon tsunami, with the erosion of peaty and silty bottom layers and the deposit of a thin bioclastic sandy bed. This deposit has typical tsunami features (basal erosive surface, rip-up clasts, marine and brackish mollusc shell debris, transported foraminiferal assemblages) and represents the first faunal evidence of this tsunami in the Mediterranean Sea.

Declaration of Competing Interest

The authors declare that they have no known competing financial interests or personal relationships that could have appeared to influence the work reported in this paper.

Acknowledgements

We thank the Gibraltar National Museum and its Director, Dr. Clive Finlayson, for the efforts made to conserve and acquire the BH borehole core. In addition, we thank the review of Dr. Akihisa Kitamura and Dr. Briony Mamo, whose suggestions greatly improved the manuscript, and the associate-editor of Geobios, Dr. Frédéric Quillévéré, for his kind help and comments during the revision process. This research was supported by two postdoctoral fellows of the Spanish Ministry of Science and Innovation Government (Subprograma JDCMICINN, JCI-2010-06160) and the Huelva University (PP2010 P-01). Furthermore, this work is carried out through DGYCIT project CTM2006-06722/MAR, DGYCIT project CGL2006-01412, FEDER 2014-2020 project UHU-126029, PID2021-127268NB-I00 project funded by MCIN/ AEI /10.13039/50110 0011033/ and by FEDER, and AYUDA PUENTE 2021 project M2615 of the Rey Juan Carlos University. Other funds have come from the Andalusian Government (groups RNM-238, RNM-293 and RNM-349) and Autonomous University of Madrid (GPG-418 Research Group). It is a contribution to the Research Center in Historical, Cultural and Natural Heritage (CIPHCN) of the University of Huelva.

References

Al-Wosabi, M., Mohammed, M., Basardah, F., 2017. Taxonomy and distribution of recent benthic foraminifera from Bir Ali Beach, Shabwah Governorate, Arabian Sea, Yemen. Geological Bulletin of Turkey 60, 383–432.

Anistratenko, V.V., 2005. Lectotypes for *Tricolia pullus*, *Gibbula divaricata* and *Theodoxus fluviatilis* (Mollusca, Gastropoda) revisited. Vestnik Zoologii 39, 3–10.

Avramides, P., Iliopoulos, G., Panagiotaras, D., Papoulis, D., Lambropoulou, P., Kontopoulos, N., Siavales, G., Christanis, K., 2014. Tracking Mid- to Late Holocene depositional environments by applying sedimentological, palaeontological and geochemical proxies, Amvrakikos coastal lagoon sediments, Western Greece, Mediterranean Sea. Quaternary International 332, 19–36.

Baptista, M.A., Heitor, S., Miranda, J.M., Miranda, M.A., Victor, L.M., 1998. The 1755 Lisbon tsunami: Evaluation of the tsunami parameters. Journal of Geodynamics 25, 143–157.

Bourgueois, J., 1994. Tsunami deposits and the K/T boundary: A sedimentologisťs perspective. LPI Contribution 825, 16–17.

Bourgueois, J., 2009. Geological effects and records of tsunamis. In: Robinson, A.R., Bernard, E.N. (Eds.), The Sea, vol. 15. Harvard University Press, Tsunamis, pp. 53–91.

Chagué-Goff, C., Schneider, J.-L., Goff, J.R., Dominey-Howes, D., Strotz, L., 2011. Expanding the proxy toolkit to help identify past events-Lessons from the 2004 Indian Ocean Tsunami and the 2009 South Pacific Tsunami. Earth-Science Reviews 107, 107–122.

Chagué-Goff, C., Szczucinski, W., Shinozaki, T., 2017. Applications of geochemistry in tsunami research: A review. Earth-Science Reviews 165, 203–244.

Chevalier, M., Pye, S., Porter, J., Chambers, S., 2014. Hydrobiidae on North Uist. Scottish Natural Heritage, Commissioned Report No. 559, 16 p.

Coleman, P.J., 1968. Tsunamis as geological agents. Journal of the Geological Society of Australia 15, 267–273.

Coleman, P.J., 1978. Tsunami sedimentation. In: Fairbridge, R.W., Bourgueois, J. (Eds.), Encyclopedia of Sedimentology. Dowden, Hutchinson and Ross, Stroudsburg, PA, pp. 828–832.

Costa, P.J.M., Andrade, C., 2020. Tsunami deposits: Present knowledge and future challenges. Sedimentology 67, 1189–1206.

Costa, P.J.M., Andrade, C., Freitas, M.C., Oliveira, M.A., Lopes, V., Dawson, A.G., Moreno, J., Fatela, F., Jouanneau, J.-M., 2012. A tsunami record in the sedimentary archive of the central Algarve coast, Portugal: Characterizing sediment, reconstructing sources and inundation paths. The Holocene 22, 899–914.

Cuven, S., Paris, R., Falvard, S., Miot-Noirault, E., Benbakkar, M., Schneider, J.-L., Billy, I., 2013. High-resolution analysis of a tsunami deposit: Case-study from the 1755 Lisbon tsunami in southwestern Spain. Marine Geology 337, 98–111.

Dawson, A.G., 1994. Geomorphological effects of tsunami run-up and backwash. Geomorphology 10, 83–94.

Dawson, A.G., 1996. The geological significance of tsunamis. Zeitschrift Geomorphologie 102, 199–210.

Dawson, A.G., 2003. Book review: Tsunami the Underrated Hazard. Journal of Quaternary Science 18, 581–582.

Dawson, A.G., Hindson, R., Andrade, C., Freitas, C., Parish, R., Bateman, M., 1995. Tsunami sedimentation associated with the Lisbon earthquake of 1 November AD 1755: Boca do Rio, Algarve, Portugal. The Holocene 5, 209–215.

Dawson, A.G., Stewart, I., 2007. Tsunami deposits in the geological record. Sedimentary Geology 200, 166–183.

Debenay, J.-P., Bénéteau, E., Zhang, J., Stouff, V., Geslin, E., Redois, F., Fernández-González, M., 1998. *Ammonia beccarii* and *Ammonia tepida* (Foraminifera): Morphofunctional arguments for their distinction. Marine Micropaleontology 34, 235–244.

Dezileau, L., Pérez-Ruzafa, A., Blanchemanche, P., Degeai, J.-P., Raji, O., Martinez, P., Marcos, C., Von Grafestein, U., 2016. Extreme storms during the last 6500 years from lagoonal sedimentary archives in the Mar Menor (SE Spain). Climate of the Past 12, 1389–1400.

Donadio, C., Paliaga, G., Radke, J.D., 2020. Tsunamis and rapid coastal remodeling: Linking energy and fractal dimension. Progress in Physical Geography: Earth and Environment 44, 550–571.

Dura, T., Hemphill-Hale, E., 2020. Diatoms in tsunami deposits. In: Engel, M., May, S. M., Pilarczyk, J., Brill, D., Garrett, E. (Eds.), Geological Records of Tsunamis and Other Extreme Waves. Elsevier, pp. 291–322.

El Talibi, H., El Moussaour, S., Zagloul, M.N., Aboumaria, K., Wassmer, P., Mercier, J.-L., 2016. New sedimentary and geomorphic evidence of tsunami flooding related to an older event along the Tangier-Asilah coastal plain, Morocco. Geoenvironmental Disasters 3, 14.

Engel, M., May, S.M., Pilarczyk, J., Brill, D., Garrett, E., 2020. Geological record of tsunamis and other extreme waves: Concepts, applications and a short history or research. In: Engel, M., May, S.M., Pilarczyk, J., Brill, D., Garrett, E. (Eds.), Geological Records of Tsunamis and Other Extreme Waves. Elsevier, pp. 3–20.

Finger, K.L., 2018. Tsunami-generated rafting of foraminifera across the North Pacific Ocean. Aquatic Invasions 13, 17–30.

Fiorini, F., 2004. Benthic foraminiferal associations from Upper Quaternary deposits of southeastern Po Plain, Italy. Micropaleontology 50, 45–58.

Font, E., Veiga-Pires, C., Pozo, M., Nave, S., Costa, S., Ruiz, F., Abad, M., Simoes, N., Duarte, S., Rodríguez Vidal, J., 2013. Benchmarks and sediment source(s) of the 1755 tsunami deposit at Boca do Rio Estuary. Marine Geology 343, 1–14.

Gómez, G., 2017. Guía de los moluscos marinos de Huelva y del Golfo de Cádiz. Diputación de Huelva, colección Divulgación.

González-Regalado, M.L., Ruiz, F., Baceta, J.I., González-Regalado, E., Muñoz, J.M., 2001. Total benthic foraminifera assemblages in the southwestern Spanish estuaries. Geobios 34, 39–51.

Guerra, L., Veiga-Pires, C., González-Regalado, M.L., Abad, M., Toscano, A., Muñoz, J.M., Ruiz, F., Rodríguez Vidal, J., Cáceres, L.M., Izquierdo, T., Carretero, M.I., Pozo, M., Monge, G., Tosquella, J., Prudencio, M.I., Dias, M.I., Marques, R., Gómez, P., Romero, V., 2020. Late Holocene benthic foraminifera of the Roman *Lacus Ligustinus* (SW Spain): A paleoenvironmental approach. Ameghiniana 57, 419–432.

Gupta, V.K., Sen, A., Pattnaik, A.K., Rastogi, G., Bhadury, P., 2019. Long-term monitoring of benthic foraminiferal assemblages from Asia's largest tropical coastal lagoon, Chilika, India. Journal of the Marine Biological Association of the United Kingdom 99, 311–330.

Hawkes, A.D., 2020. Foraminifera in tsunami deposits. In: Engel, M., May, S.M., Pilarczyk, J., Brill, D., Garrett, E. (Eds.), Geological Records of Tsunamis and Other Extreme Waves. Elsevier, pp. 239–259.

Jarochowska, E., Munnecke, A., 2015. Silurian carbonate high-energy deposits of potential tsunami origin: Distinguishing lateral redeposition and time averaging using carbon isotope chemostratigraphy. Sedimentary Geology 315, 14–28.

Kaabouben, F., Baptista, M.A., Iben Brahim, A., El Mouwraouah, A., Toto, A., 2009. On the moroccan tsunami catalogue. Natural Hazards and Earth System Sciences 9, 1227–1236. https://doi.org/10.5194/nhess-9-1227-2009.

Kitamura, A., Ito, M., Sakai, S., Yokohama, Y., Miyairi, Y., 2018. Identification of tsunami deposits using a combination of radiometric dating and oxygen-isotope profiles of articulated bivalves. Marine Geology 403, 57–61.

Kumar, P., Barnejee, M., 2016. Holocene biostratigraphic zones corresponding litho-chronostratigraphy, environment of deposition and successive changes in the geomorphology of Bengal Basin, India during last 10,000 years. International Journal of Geosciences 7, 615–629.

Lario, J., Zazo, C., Goy, J.L., Dabrio, C.J., Borja, F., Silva, P.G., Sierro, F.J., González, J.A., Soler, V., Yll, E.I., 2002. Changes in sedimentation trends in SW Iberia Holocene estuaries (Spain). Quaternary International 93–94, 171–176.

Le Roux, J.P., Nielsen, S.N., Kemnits, H., Henriquez, A., 2008. A Pliocene mega-tsunami deposit and associated features in the Ranquil Formation, southern Chile. Sedimentary Geology 203, 164–180.

Luque, L., Lario, J., Civis, J., Silva, P.G., Zazo, C., Goy, J.L., Dabrio, C.J., 2002. Sedimentary record of a tsunami during Roman times, Bay of Cadiz, Spain. Journal of Quaternary Science 17, 623–631.

Mamo, B., Strotz, L., Dominey-Howes, D., 2009. Tsunami sediments and their foraminiferal assemblages. Earth-Science Reviews 96, 263–278.

Martínez Solares, J.M., 2001. Los efectos en España del terremoto de Lisboa (1 de noviembre de 1755). Monografías IGN., 19. Instituto Geográfico Nacional, Madrid.

Matysik, M., Szulc, J., 2019. Shallow-marine carbonate sedimentation in a tectonically mobile basin, the Myschelkalk (Middle Triassic) of Upper Silesia (northern Poland). Marine and Petroleum Geology 107, 99–115.

Melis, R., 2013. Distribution and morphological abnormalities of recent foraminifera in the Marano and Grado Lagoon (North Acriatic Sea. Italy). Mediterranean Marine Sciences 14, 432–450.

Morhange, C., Goiran, J.-P., Bourcier, M., Carbonel, P., Le Campion, J., Rouchy, J.-M., Yon, M., 2000. Recent Holocene paleo-environmental evolution and coastline changes of Kition, Larnaca, Cyprus, Mediterranean Sea. Marine Geology 170, 205–230.

Murray, J., 2006. Ecology and Applications of Benthic Foraminifera. Cambridge University Press, Cambridge, New York, Melbourne.

Nagendra, R., Kamalak, B.V., Sajith, C., Sen, G., Reddy, A.N., Srinivasalu, S., 2005. A record of foraminiferal assemblage in tsunami sediments along Nagappattinam coast, Tamil Nadu. Current Science 89, 1947–1952.

Papaspyrou, S., Diz, P., García-Robledo, E., Corzo, A., Jiménez-Arias, J.L., 2013. Benthic foraminiferal community changes and their relationship to environmental dynamics in inter tidal muddy sediments (bay of Cádiz, SW Spain). Marine Ecology Progress Series 490, 121–135.

Paris, R., Cachao, M., Fournier, J., Voldoire, O., 2010. Nannoliths abundance and distribution in tsunami deposits: Example from the December 26, 2004 tsunami in Lhok Nga (northwest Sumatra, Indonesia). Géomorphologie 16, 109–118.

Pilarczyk, J.E., Dura, T., Horton, B.P., Engelhart, S., Kempo, A.C., Sawai, Y., 2014. Microfossils from coastal environments as indicators of paleoearthquakes, tsunamis and storms. Palaeogeography, Palaeoclimatology, Palaeoecology 413, 144–157.

Pilarczyk, J.E., Sawai, Y., Matsumoto, D., Namegaya, Y., Nishida, N., Ikehara, K., Fujiwara, O., Gouramanis, C., Dura, T., Horton, B.P., 2019. Constraining sediment provenance for tsunami deposits using distributions of grain size and foraminifera from the Kujukuri coastline and shelf, Japan. Sedimentology 67, 1373–1392.

Prastowo, T., Cholifah, L., Ngkoimani, L.O., Saffiuddin, L.O., 2017. Tsunami-magnetic signals and magnetic anomaly generated by tsunami wave propagation at open sea. Indones. Journal of Physical Education 13, 59–70.

Quintela, M., Costa, P., Fatela, F., Drago, T., Hoska, N., Andrade, C., Freitas, M.C., 2016. The AD 1755 tsunami deposits onshore and offshore of Algarve (south Portugal): Sediment transport interpretations based on the study of Foraminifera assemblages. Quaternary International 408, 123–138.

R-core team, 2019. R: A Language and Environment for Statistical Computing. R Foundation for Statistical Computing, Vienna, Austria.

Rodríguez-Vidal, J., Cáceres, L.M., Abad, M., Ruiz, F., González-Regalado, M.L., Finlayson, C., Finlayson, G., Fa, D., Rodríguez-Llanes, J.M., Bailey, G., 2011. The recorded evidence of AD 1755 Atlantic tsunami on the Gibraltar coast. Journal of Iberian Geology 37, 177–193.

Rose, E.P.F., Rosenbaum, M.S., 1990. Royal Engineer geologists and the geology of Gibraltar. Royal Engineer Journal 104, 128–144.

Ruiz, F., Rodríguez Ramírez, A., Cáceres, L.M., Rodríguez Vidal, J., Carretero, M.I., Clemente, L., Muñoz, J.M., Yáñez, C., Abad, M., 2004. Late Holocene evolution of the southwestern Doñana National Park (Guadalquivir Estuary, SW Spain): A multivariate approach. Palaeogeography, Palaeoclimatology, Palaeoecology 204, 47–64.

Ruiz, F., Rodríguez Ramírez, A., Cáceres, L.M., Rodríguez Vidal, J., Carretero, M.I., Abad, M., Olías, M., Pozo, M., 2005. Evidence of high-energy events in the geological record: Mid-Holocene evolution of the southwestern Doñana National Park (SW Spain). Palaeogeography, Palaeoclimatology, Palaeoecology 229, 212–229.

Ruiz, F., Abad, M., Rodríguez Vidal, J., Cáceres, L.M., González-Regalado, M.L., Carretero, M.I., Pozo, M., Gómez Toscano, F., 2008. The geological record of the oldest historical tsunamis in southwestern Spain. Rivista Italiana di Paleontologia e Stratigrafia 114, 147–156.

Ruiz, F., Abad, M., Cáceres, L.M., Rodríguez Vidal, J., Carretero, M.I., Pozo, M., González-Regalado, M.L., 2010a. Ostracods as tsunami tracers in Holocene sequences. Quaternary International 73, 130–135.

Ruiz, F., Pozo, M., Carretero, M.I., Abad, M., González-Regalado, M.L., Pichardo, M., Rodríguez Vidal, J., Cáceres Puro, L.M., Pendón, J.G., Prudêncio, M.I., Dias, M.I., 2010b. Birth, Evolution and Death of a Lagoon: Late Pleistocene to Holocene Palaeoenvironmental Reconstruction of the Doñana National Park (SW Spain). In: Friedman, A.G. (Ed.), Lagoons: Biology, Management and Environmental Impact. Nova Science Publishers, New York, pp. 371–396.

Ruiz, F., Rodríguez Vidal, J., Abad, M., Cáceres, L.M., Carretero, M.I., Pozo, M., Rodríguez-Llanes, J.M., Gómez, F., Izquierdo, T., Font, E., Toscano, A., 2013. Sedimentological and geomorphological imprints of Holocene tsunamis in Southwestern Spain: An approach to establish the recurrence period. Geomorphology 203, 97–104.

Silva, P.G., Gómez-Diego, P.V., Elez, J., Giner-Robles, J.L., Rodríguez-Pascua, M.A., Roquero, E., Martínez-Graña, A., Bardají, T., Bautista, B., 2017. Earthquake Environmental Effect of the AD 1755 Lisbon Earthquake-tsunami in Spain. Actas IX Reunión Cuaternario Ibérico, Faro, pp. 53–57.

Solares, J.M.M., Arroyo, A.L., 2004. The great historical 1755 earthquake. Effects and damage in Spain. Journal of Seismology 8, 1–275.

Templado, J., 2011. Familia Trochidae. In: Gofas, S., Moreno, D., Salas, C. (Eds.), Moluscos marinos de Andalucía. Universidad de Málaga, Málaga, pp. 104–117.

Tohver, E., Schmieder, M., Lana, C., Mendes, P.S.T., Jourdan, F., Warren, L., Riccomini, C., 2018. End-Permian impactogenic earthquake and tsunami deposits in the intracratonic Paraná Basin of Brazil. GSA Bulletin 130, 1099–1120.

Villanueva, P., 1995. Implicaciones oceanograficas de los foraminiferos bentonicos recientes en la bahia y plataforma gaditana. Taxonomia y asociaciones. Ph.D. Thesis, Universidad de Cádiz (unpubl.).

Whelan, F., Kelletat, D., 2005. Boulder deposits on the southern Spanish Atlantic coast: Possible evidence for the 1755 AD Lisbon Tsunami? Science of Tsunami Hazards 23, 25–38.

Zazo, C., Goy, J.L., Somoza, L., Dabrio, C.J., Belloumini, G., Improta, S., Lario, J., Bardají, T., Silva, P.G., 1994. Holocene sequence of sea-level fluctuations in relation to climatic trends in the Atlantic-Mediterranean linkage coast. Journal of Coastal Research 10, 933–945.